JOURNAL OF PROPULSION AND POWER
Vol. 9, No. 5, Sept.–Oct. 1993

Validation Studies of Scramjet Nozzle Performance

Tohru Mitani,* Shuichi Ueda,† Koichiro Tani,‡ Shigeru Sato,§ and Hiroshi Miyajima¶
National Aerospace Laboratory, Kakuda Research Center, Kimigaya 1, Kakuda, Miyagi 981-15, Japan
and
Masashi Matsumoto** and Shouhachi Yasu††
Ishikawajima-Harima Heavy Industry Co., Ltd., Tonogaya 1, Mizuho, Nishitama, Tokyo 190-12, Japan

Thrust by scramjet nozzles was measured using a high-temperature gas flow with Mach 2.5 and a total temperature of 3100 K by combustion of monomethyl-hydrazine (MMH) and nitrogen tetraoxide (NTO). Wall pressure on the nozzles was monitored to estimate the pressure force on the nozzles. Series of cold nitrogen (N_2) flow tests were also conducted using the same nozzles. An inviscid two-dimensional code was able to reproduce nozzle performance of the cold N_2 flow. The calculations with chemical kinetics also predicted the experimental results of the MMH/NTO flow within an error of 3.6%. Kinetic, two-dimensional and friction losses in the scramjet nozzles were identified for the nozzle, and the scale effects of the nozzle performance of H_2-fueled engines are discussed.

I. Introduction

FOR a space plane driven by scramjet engines, requirements of propulsion, aerodynamics, and structure necessitate airframe-integrated engines. In which case, the forebody works as the precompression part for the inlet and the afterbody acts as the external nozzle for the scramjet engine. Therefore, the nozzle for scramjet engines must be rectangular and asymmetric.[1,2] Hypersonic propulsion, especially in scramjets, is greatly handicapped by the ram drag. The ratio of gross thrust to net thrust increases from 1 in conventional air breathing engines to almost 10 in scramjet engines.[3] This enhances the relative significance of nozzle studies in these types of propulsion systems.

The most prominent features of the scramjet nozzle flow are the effects of nonequilibrium chemistry in high-speed nozzle flow and nonuniformity of the incoming flow from the combustor.[4] It has been reported that these factors affect the lift thrust delivered by asymmetric nozzles as well as the main thrust.[1–6] Accurate estimation of performance of the nozzle is the most essential step in the development of scramjet engines.

Because of the difficulties and limitations involved in ground-based testings of scramjets, the use of computational fluid dynamics (CFD) is essential. There have been some numerical studies on scramjet nozzles.[7–10] Harloff and Lai[7] calculated two- and three-dimensional flows of scramjet nozzles in a range of freestream Mach numbers from 3 to 14. Wall pressure, skin friction, and heat transfer rates were computed using a Navier-Stokes (PARC3D) code assuming a constant specific heat ratio. Wall pressure was compared with that measured in experiments. Recently, Huebner and Tatum[10] presented a scramjet exhaust flow simulation including the effects of inlets.[10] They compared their results with schlieren photographs and discussed the effect of a wind-off environment in ground testings.

There have, however, been relatively few experimental studies conducted for code calibrations. Most of these experimental studies have employed substitute cold gases to simulate hot combustion gases,[3,11–13] except for studies employing a detonation tube.[14] The most peculiar aspects of nozzle flow in scramjet nozzles, such as the effects of chemical nonequilibrium, can not be investigated in such cold flow experiments. It is reported that overall system performance in scramjets is very sensitive to internal skin friction.[15] The important performance criterion—thrust—has neither been measured nor have comprehensive investigations on various losses been reported.

For the purpose of establishing experimental techniques and validating engineering and analytical codes for scramjet nozzles, a series of experiments was performed under Mach 8 flight conditions using a high-temperature gas flow.[16] Thrust produced by an asymmetric nozzle was measured using load cells in high altitude conditions. Static pressure distributions on ramp and cowl walls were also measured to calculate thrust by the wall pressure. The pressure thrust was compared with the thrust measured by the load cells. The thrust performance and measured results of pitot and static pressure were compared with calculations using a two-dimensional chemical kinetic code. Losses in the nozzle flows were identified and several parameters governing the losses are discussed.

II. Experiments

A gas generator (GG) burning MMH/NTO was adopted to produce high temperature. The major reason for using these propellants was to enable accurate measurement of a relatively small increment of thrust due to the scramjet nozzles. Use of these propellants makes it possible to use the compact feed system, thus minimizing interference with the thrust measuring system indicated as TMS in Fig. 1.

The combustor consists of an injector with acoustic cavities to prevent combustion instability, and a de Laval nozzle to accelerate the combustion gas flow to Mach 2.5. The cross section of the combustor is rectangular. The dimension at the exit of the gas generator is 32 × 147.3 mm and the throat height is 8.0 mm. The length of the gas generator is 260 mm. The stagnation temperature was designed to be 3100 K, and the stagnation pressure to be 1 MPa. The static temperature and pressure at the exit of gas generator were 2100 K and 0.05 MPa, respectively. The internal nozzle was designed to

Received April 30, 1992; presented as Paper 92-3290 at the AIAA/SAE/ASME/ASEE 28th Joint Propulsion Conference and Exhibit, Nashville, TN, July 6–8, 1992; revision received March 8, 1993; accepted for publication April 14, 1993.

*Head, Ramjet Combustion Laboratory. Member AIAA.
†Researcher, Rocket Altitude Performance Laboratory.
‡Researcher, Ramjet Performance Laboratory.
§Researcher, Ramjet Combustion Laboratory.
¶Director General. Member AIAA.
**Researcher, Research Institute.
††Section Manager, Aero-Engine and Space Operations.

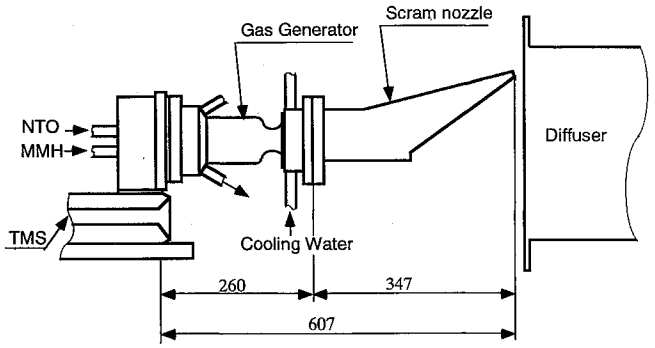

Fig. 1 Scramjet nozzle and thrust measuring system in a vacuum cell.

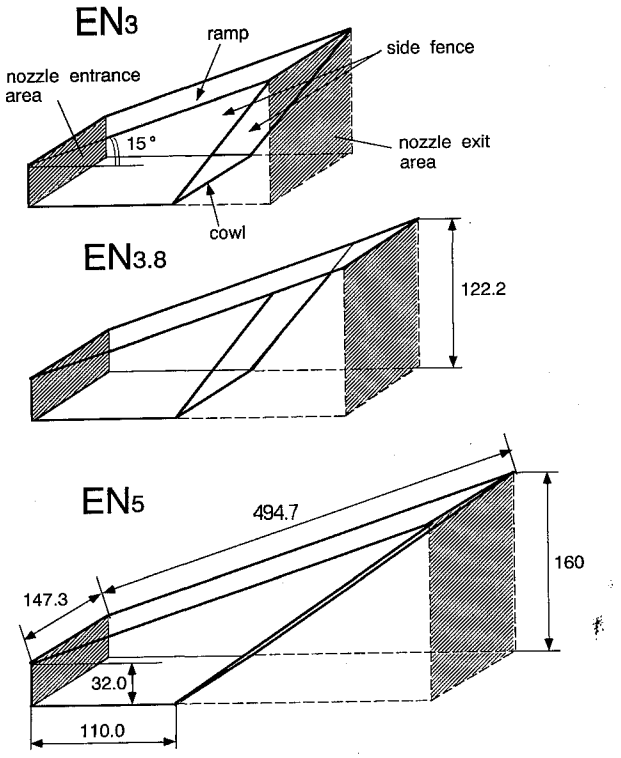

Fig. 2 Geometry of the scramjet nozzles examined (unit: mm).

be representative of the scramjet operation at the flight Mach number of 8. The configuration of the nozzle was designed to be wave-free using the method of characteristics with a correction that accounted for the displacement thickness of the boundary layer. The approximate geometry of the internal nozzle in the gas generator can be found in Figs. 5 and 10.

A simple configuration using plane walls was adopted for the scramjet nozzle in this experiment. The ramp, corresponding to the afterbody of airframe, was inclined by 15 deg to the axis of the GG. And the cowl was parallel to the GG. Configurations of scramjet nozzles examined are illustrated in Fig. 2. Two side-fences were installed in the nozzles with expansion ratios of 3 (external nozzle: EN3) and 5 (EN5) to minimized three-dimensional effects. The nozzle (EN3.8) was used to assess the effects of three-dimensional expansion of nozzle flow caused by the shorter side fences. The expansion ratio of the scramjet nozzle was defined by a ratio between the projected area in the axis of the GG and the entrance area of the scramjet nozzle. This definition is the most suitable choice for these experimental conditions, unless the wave emerging from the cowl end interacts with the nozzle ramp. The EN5 nozzle approximately corresponds to an optimum nozzle with an exhaust area to air capture area ratio of 1.5 in airframe-integrated scramjets, which was indicated by Snyder and Pinckney.[2] The configuration of the gas generator and the EN3.8 scramjet nozzle is shown in Fig. 1.

The experiments were conducted using a thrust measuring system installed in a high-altitude test stand at the National Aerospace Laboratory, Kakuda Research Center (KRC). This facility can simulate high-altitude conditions from $\frac{1}{30}$ to $\frac{1}{200}$ atmospheric pressure for 180 s by a steam ejector system. This high-altitude condition corresponds to the nozzle pressure ratio (NPR) of 10^3 or higher for the combustion pressure of 1 MPa. Effects of NPR are also being investigated in this series of experiments using the cold N_2 flow.[17] However, only the experiments in underexpansion for the scramjet nozzles and in the wind-off environment are presented here.

The wall pressure was measured at 150 stations distributed on the walls of scramjet nozzles using three scanning pressure sensors. Because precise measurements of velocity profiles are difficult for a hot gas flow with a total temperature of 3100 K, friction was estimated from heat flux measurements. Heat transfer rates in the scramjet nozzles were measured using thermocouples and heat flux meters. Heat flux estimated by a transient method was compared with the results by the heat flux meters (Hycal Co.). The friction coefficients were reduced by using the Reynolds analogy assuming a weak pressure gradient in the flow direction.

Precise measurement of the incoming flow to the nozzle is an essential step to investigate the performance of nozzles. Since it is difficult to measure the high-temperature flow, experiments using N_2 flow with the same nozzle were performed. Pitot pressure, static pressure, and total temperature were measured using fine probes of 0.5-mm diameter. The flowfield was visualized by shadowgraph and schlieren photographs.

III. Experimental Results

Table 1 summarizes the thrusts measured in MMH/NTO firing tests. Since the thrust is dependent on combustion pressure, oxidizer/fuel ratio, and throat area, a reduced value at the reference condition was calculated to correct these variations in each experimental run. In addition, the measured thrust was corrected for environmental pressure to obtain the vacuum thrust, as is commonly done in the evaluation of rocket performance. The measurements revealed the thrust delivered by the GG to be 1.79 kN, and that measured with the scramjet nozzle EN3 to be 1.91 kN. This shows the increment of thrust by the scramjet nozzle to be 122 N. In-

Table 1 Thrust by load cells ($F_{\text{load cell}}$) and thrust measured from wall pressure (F_{pressure}) in Newton

	$F_{\text{load cells}}$	Increment of F	F_{pressure}
GG	1785.7	0	
GG + EN_3	1913.6	127.9	141.4
+ $EN_{3.8}$	1940.2	154.5	172.5
+ EN_5	1967.9	182.2	211.7

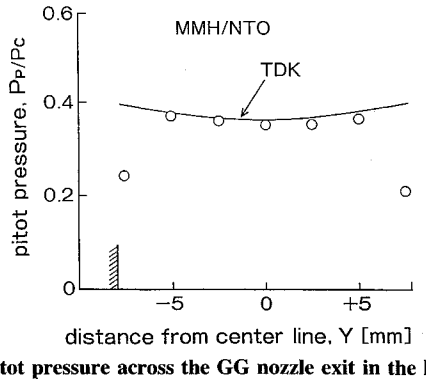

Fig. 3 Pitot pressure across the GG nozzle exit in the hot flow.

creasing the expansion ratio to 5.0 resulted in an increase of thrust delivered by the scramjet nozzle to 183 N.

The entrance conditions of the flow into the nozzles were investigated first. Pitot pressure distribution across the nozzle exit of the GG was compared with the results predicted by an inviscid two-dimensional chemical kinetic (TDK) code, described later (Fig. 3). The TDK code[18] was revised for asymmetric, plane flow to analyze scramjet nozzles. The solid line in the figure denotes the calculated results; the experimental values measured at $Y = \pm 7$ mm are affected by expansion fans originating from the nozzle exit. The measured pitot pressure was found to agree well with the calculated pressure within a discrepancy of 5%. The concave distribution of pressure was due to a mismatch in specific heat ratio evaluated for the MMH/NTO combustion gas.

Static pressure is more sensitive to flow conditions and provides a stricter parameter for evaluation than pitot pressure. Figure 4 illustrates the static pressure distribution for the cold N_2 flow measured along the centerline of the GG nozzle exit (○) and on the side wall (●). The solid line represents the calculated result. The larger value of specific heat of N_2 emphasizes the concave nature of the pressure distribution. The high static pressure in the traverse measurement near the nozzle walls is caused by a reflected compression

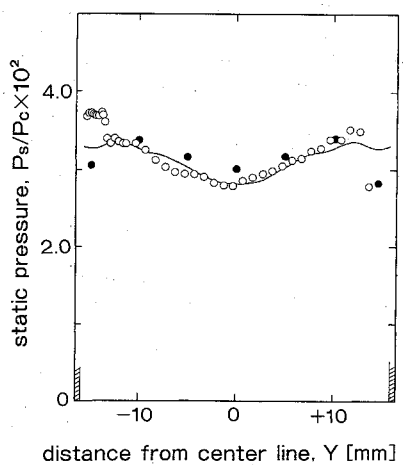

Fig. 4 Distribution of static pressure at the GG nozzle exit (cold N_2).

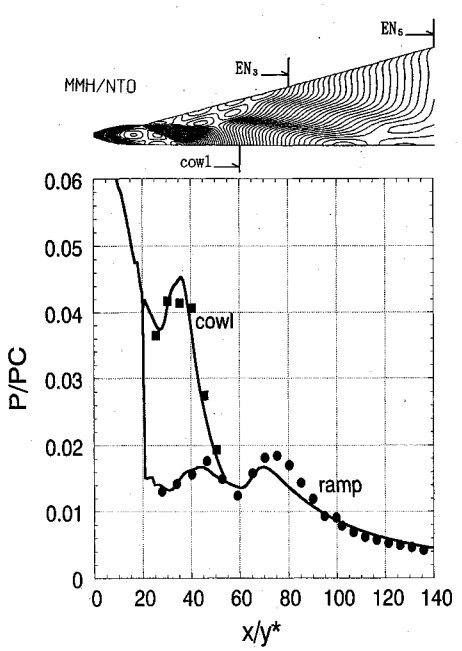

Fig. 5 Isobaric contours and nozzle wall pressure in the hot flow.

wave originating from the leading edge of the static pressure probe. The aerodynamic part of the TDK code can be examined from Fig. 4. The chemical part in the addition of the aerodynamic part of the code was validated by the comparisons in Figs. 3 and 5. Thus, the verification of the TDK code was made for application to scramjet nozzles.

An isobaric distribution of MMH/NTO combustion gas flow in the nozzle is shown in the upper part of Fig. 5, which was calculated by the TDK code. A Prandtl-Meyer expansion wave is initiated from the ramp corner, and some high-/low-pressure islands are observed in the flowfield caused by nonuniformity of gas flow from the GG nozzle. Figure 5 also illustrates the static pressure distributions on the ramp and cowl walls. The pressure is nondimensionalized using the chamber pressure (P_c). The distance from the throat of the GG has also been normalized by the half-height of the throat in the GG ($Y^* = 4.0$ mm).

Comparison with the isobaric contours in Fig. 5 shows that the ramp pressure decreases to 0.013 around the ramp corner and that the cowl pressure maintains the pressure at the GG nozzle exit (0.04). The cowl pressure decreases from $X/Y^* = 35$ by the incidence of the expansion wave from the ramp. The reflected wave now incident on the ramp wall at $X/Y^* = 70$ decreases the ramp pressure. The two solid lines are the results predicted by the TDK. The results reveal correct variations of pressure, though the steepness of the pressure variations caused by the nonuniformity of flow deteriorates in the calculation.

Using the cold N_2 flow, the boundary layer developed on the scramjet nozzle was measured. Figure 6 shows the velocity profiles at the GG exit (●), and the EN3 (△) and EN5 nozzle exits (□). The coordinate Y is normalized by the local momentum thicknesses (δ_2). The freestream velocity (U) is calculated using the TDK code. The figure implies that the ve-

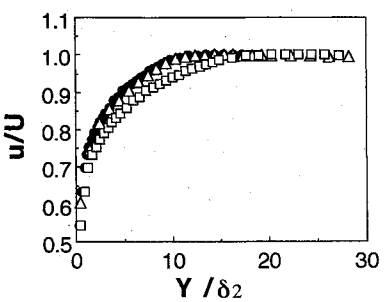

Fig. 6 Velocity profiles in the boundary layers measured in the cold N_2 flow.

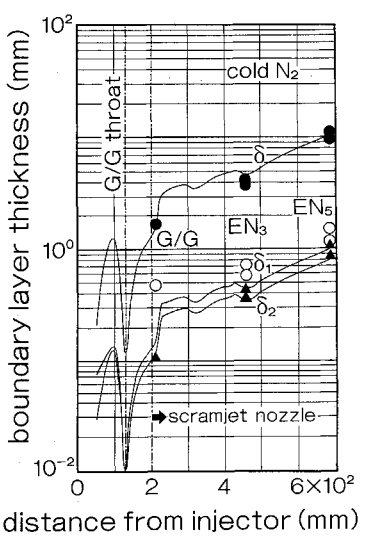

Fig. 7 Development of the boundary-layer thicknesses (cold N_2).

locity profiles are similar with respect to nozzle locations and that the boundary layers are turbulent. The $\frac{1}{7}$th-power law profile could be compared in Fig. 6, though the line was found to be hardly distinguishable from the symbols □.

The thickness of the boundary layer (δ) developed in the nozzle is 1.8 mm at the exit of the GG and thickens to 11 mm at the exit of the EN5 nozzle as shown in Fig. 7. This thickness, as well as the displacement thickness (δ_1) and the momentum thickness (δ_2), was evaluated using an integral method.[19] Figure 7 shows good agreement between the calculated values (solid lines) and the thicknesses measured at the exits of the GG nozzle, the EN3, and EN5 nozzles.

IV. Discussion

A. MMH/NTO Experiments

A method for evaluating performance of liquid propellant rockets has been established by JANNAF[20,21] and adopted here. The performances of nozzles are illustrated in Fig. 8, in which the calculated *Isp* is compared with the *Isp* obtained by the pressure integral (denoted by $\int PdA$) and the *Isp* measured by the load cells (F). Four computer codes, one-dimensional equilibrium (ODE), one-dimensional chemical kinetic (ODK), two-dimensional chemical kinetic (TDK) and boundary layer (BL) codes, were run in this study. The ODE and ODK codes are based on the JANNAF codes.

The TDK was prepared in the KRC to evaluate performance of liquid propellant rockets. The inviscid TDK code uses the MacCormack scheme for streamwise marching in the core flow in nozzles, in which the convection terms for conservative variables are discretized explicitly and the chemical source terms are treated implicitly. The reaction model used in this study includes a set of 24 elementary reactions with their backward reactions for 12 species for the C-H-O-N system. The rate constants and the third-body efficiencies were chosen from the data in Refs. 22–24. Assuming chemical equilibrium at the entrance of the contraction part of GG, the chemical kinetics are tracked down in the expansion section of the GG and the scramjet nozzles. The details and the code validation studies are described in Refs. 18 and 21.

The friction loss in nozzles was assessed using the BL code, in which chemically inert, two-dimensional boundary layers was assumed. Davis et al.[25] investigated supersonic turbulent flow development in a square duct using a uniform flow with a Mach 3.9 and the unit Reynolds number of 20×10^6/m. Their experimental study indicated that the boundary layer at the corner bisector is thicker than the boundary layer along the wall bisector, but the influence of the corner flow is confined into the narrow corner regions for the large Reynolds number. The boundary layer must be thinner in the accelerated flow in our nozzles than in the duct with a constant area. Thus, the three-dimensional effects caused by the presence of the side fences were neglected in the calculations. The pitot pressure distribution measured at 182 locations in the cross section of the GG exit also supported this conclusion.

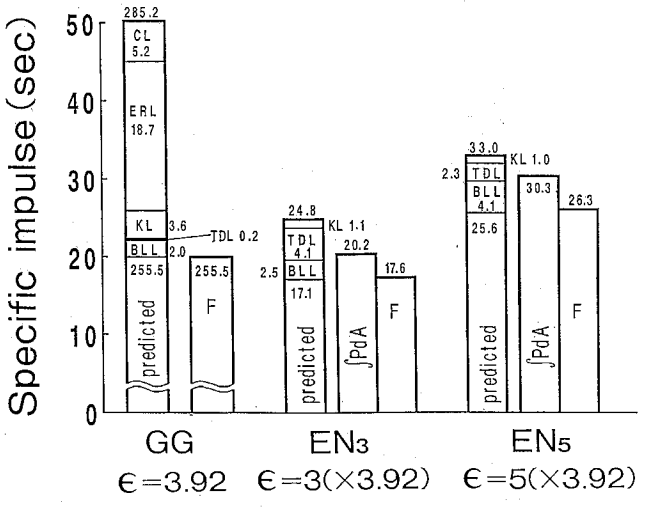

Fig. 8 Nozzle performance in the hot MMH/NTO flow.

In this study, the momentum integral method proposed by Spalding and Chi[19] was adopted for estimation of the development of the boundary layer, because the integral methods have been calibrated by many experiments using various wind tunnels.[26] Integral methods are employed in the JANNAF thrust loss calculation method,[20,21] and the effects of transverse and longitudinal curvature have recently been included to assess viscous loss in rocket engines.[27] Recently, Hedlund et al.[28] carried out the Mach 8 calibration test of the Naval Surface Warfare Center, hypervelocity wind tunnel no. 9. They reported that Van Driest's method predicted the heat transfer rates very well, whereas a viscous code underpredicted the data by 7–12%. Two- and three-dimensional viscous calculations for our nozzle experiments are also performed using a second-order accurate TVD scheme and a fourth-order accurate scheme, called the KRC code,[29] developed in our laboratory. Comparison with various schemes and the experimental results will be presented at another time.

A part of thermal energy may be released by recombination of radicals near the nozzle walls to recover the chemical kinetic loss in the nozzle flow. However, this increase of the nozzle performance might be small, because the chemical kinetic loss in the core flow of nozzles is dominant. The order of magnitude of quenching rate of radicals in the boundary layer can be easily expressed by using the displacement thickness, if all the radicals entrained in the boundary layer are postulated to be terminated at the nozzle walls. The recovery rate of the kinetic loss in the boundary layer was estimated to be less than 1% of the kinetic loss produced in the core flow in our subscale experiment, if the displacement thickness (1 mm) is compared with the height of the core flow (150 mm). The effect could be negligible in full-scale engines, since the relative thickness of the boundary layer decreases as increasing the nozzle dimensions. Therefore, the chemical reactiveness in the boundary layer was neglected in the BL code to evaluate the nozzle performance.

The difference between ODE and ODK corresponds to the chemical kinetic (nonequilibrium) loss (KL) in nozzles, and the difference between ODK and TDK denotes the two-dimensional (divergence) loss (TDL). The difference between the two experimental results, the thrust measured by the load cell, and the thrust integrating wall pressure, represents the friction loss acting on scramjet nozzles (BLL).

In order to discuss nozzle performance driven by the MMH/NTO combustion gas, one has to evaluate total temperature (energy release efficiency) in the GG first. Defining cooling loss (CL), nonequilibrium loss (KL), two-dimensional loss (TDL) and friction loss in the boundary layer (BLL) in the GG, the combustion efficiency (ER) can be estimated from the measured specific impulse (Isp_{msd}) as

$$\mathrm{ER} = Isp_{msd}/(Isp_{ode}\text{-CL-KL-TDL-BLL})$$

where Isp_{ode} denotes the specific impulse (*Isp*) given by chemical equilibrium calculations. The temperature increment of cooling water and the measured thrust of GG yielded a combustion efficiency of 93.0%, and the total energy release efficiency including cooling loss was evaluated to be 91.3%. These evaluations were found to be consistent with the measured nozzle pressure of GG.

The result shown on the far left in Fig. 8 is that for the GG. Complete burning and equilibrium yields an *Isp* of 285.2 s. In addition to the energy release loss of 19.1 s, the KL was calculated to be 3.6 s and the TDL to be negligible. A laminar boundary layer was postulated for the hot combustion gas and the BLL was evaluated to be 2.0 s. The TDK calculation

shows that the two-dimensional loss increases in the EN3 nozzle (16.5%) and recovers in the EN5 nozzle (7.0%), because the flow is rectified in the downstream region of scramjet nozzles. This large TDL is due to the simple configuration of the ramp adopted in this study. The KL was found to be 4.5% in EN3 and EN5 nozzles. The calculated *Isp* can be compared with the *Isp* of the core flow evaluated after integration of the wall pressure. The calculated values of 19.7 s (EN3) and 29.9 s (EN5) agree with the experimental ones within a difference of 5%.

B. Friction Loss in Scramjet Nozzles

A turbulent boundary layer was assumed in the scramjet nozzles for the hot gas flow with the unit Reynolds number of 0.5×10^6. The friction loss (BLL) was estimated to be 2.5 s (EN3) and 4.1 s (EN5) in Fig. 8. The friction losses in EN3 and EN5 nozzles were experimentally evaluated to be 3 s and 4.3 s, respectively. In the figure, predicted values of *Isp* agree with experimental values obtained by the thrust measurements within a discrepancy of 2%.

Figure 9 shows the nozzle performance measured in the cold N_2 flow using the same nozzles. The delivered *Isp* of GG agreed with the predicted value within a discrepancy of 0.7%, if the real-gas effect of N_2 was considered for the density calculation. Predicted performance differs from the experimental performance by 1.3% in EN3 and 6.5% in EN5, respectively. The present calculations underpredicted the delivered *Isp* by 24%, if the BLL is included.

Most of the error is due to the difficulty in discussing the small increments after subtraction of large values including thrust by the GG in the experiments. Accuracy of force measurements restricts precise assessment of boundary-layer loss. This problem becomes especially serious, when the friction loss (BLL) is elucidated by the small difference between the pressure thrust and the load-cell thrust. Therefore, independent measurement of the boundary layer is essential for nozzle research. Direct measurements of boundary-layer thicknesses in the hot flow are necessary for evaluating the accurate friction loss.

C. Parameters Governing Nozzle Performance

After the calibration studies of the computer codes, size effect of performance of H_2-fueled scramjet nozzles was investigated. The tested nozzle contour is shown in Fig. 10, in which the ramp with an EN5 has an initial ramp angle of 18 deg and is optimized using a method proposed by Nickerson.[30] The performance was calculated assuming the stoichiometric burning of H_2 with the air (the total temperature of 2600 K). The large value of *Isp* by two orders of magnitude in Fig. 10 is due to the value based on the fuel (H_2) flow rate rather than the total flow rate of propellants in Fig. 8. The two-dimensional loss in diverging nozzle flow has no scale-dependence. The scale effects of the chemical KL can be expressed in terms of the Damkoelar numbers and that of the friction loss appears through Reynolds number. The extrapolation of KL in the core flow is relatively easy because the core flow does not depend on the nozzle dimensions.

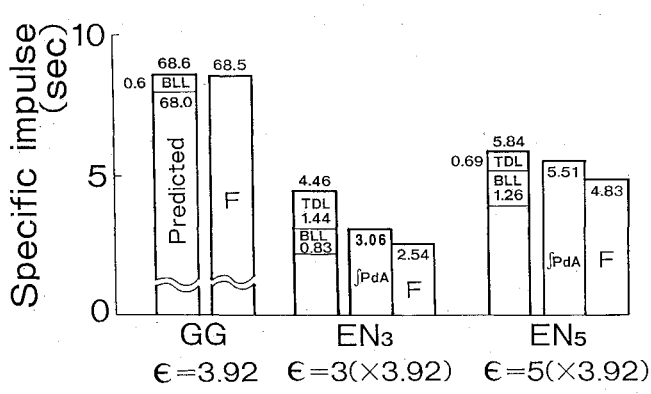

Fig. 9 Nozzle performance in the cold N_2 flow.

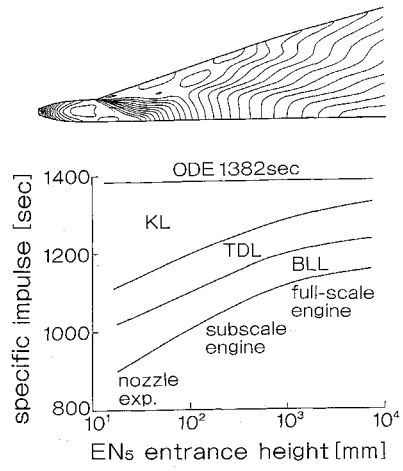

Fig. 10 Scale effects of nozzle performance (H_2-fueled scramjet nozzle).

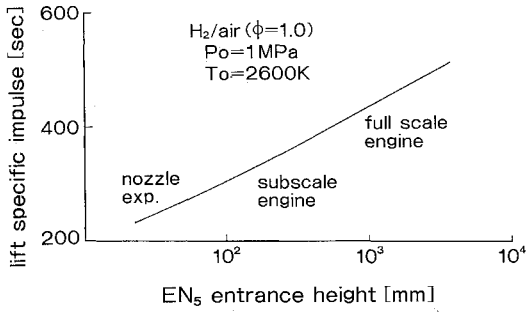

Fig. 11 Scale effect of lift thrust caused by the finite-rate chemistry.

The most crucial problem in the scale effect of the friction loss (BLL) is the laminar/turbulent transition and the relaminarization in nozzles. Because of the low viscosity of the cold N_2, the unit Reynolds number in the present experiments was evaluated to be 20×10^6/m, which coincides to the Reynolds number for the full-scale engines with the nozzle entrance height of 1 m. The measurements of heat transfer rates expelled the possibility of the laminar/turbulent transition in the range of the Reynolds number in Fig. 10. Thus, the turbulent boundary layer was assumed from the present nozzles experiment to the full-scale engines.

The *Isp* given by ODE (1382 s) is reduced by the kinetic loss, the two-dimensional loss, and the friction loss. The KL decreases with the nozzle dimensions because the longer residence time in the nozzles shifts the reactive flow to chemical equilibrium. It was found that these three losses were approximately equal in full-scale engines with an entrance height of 1 m. The figure indicates the *Isp* delivered by the scramjet nozzle to be approximately 1100 s.

The scale effect of lift thrust by the scramjet nozzle revealed that a full-size nozzle delivers lift thrust three times as great as the thrust in the subscale nozzle with a nozzle height of 40 mm as shown in Fig. 11. The kinetic loss increases by a factor of 3 as the total pressure decreases from 1 to 0.1 MPa. The ODK calculations demonstrated that H atoms and OH radicals are responsible for the kinetic loss in scramjet nozzles. An interesting feature is that the concentration of H atoms decreases near the throat of the GG, but then increases downstream in the scramjet nozzles. Detailed studies on chemical kinetics in scramjet nozzles elucidated that the concentration of H atoms is determined by the partial equilibrium in an overall branching reaction

$$3H_2 + O_2 = 2H_2O + 2H$$

and that the concentrations of radicals, OH and O can be written in terms of the concentrations of stable species and the H atoms.

The peculiar increase of H atoms downstream and the dependence of chemical kinetic loss in nozzles on the stoichiometry could be interpreted by the partial equilibrium. The results indicate that chemical kinetic loss in scramjet nozzles is dominated by $H + O_2 + M$ reaction in fuel-lean conditions and by $H + OH + M$ and $H + H + M$ reactions in fuel-rich conditions.

The partial equilibrium becomes more dominant in scramjet nozzles, because radical-branching reactions overcome radical-breaking reactions in flight with a high Mach number and a low nozzle pressure. Using the approximation of partial equilibria in chemistry, the reactive flow in scramjet nozzles could be expressed by an overall reduced kinetic model consisting of various radical breaking reactions.

V. Conclusions

1) An inviscid two-dimensional, chemical kinetic (TDK) code was adopted to predict nozzle performance, and the results were compared with experiments using a hot MMH/NTO combustion gas flow of 3100 K and a cold N_2 flow. Maximum discrepancies between calculations and experiments were 3.6% (hot flow) and 6.6% (cold flow) for the core flow performance.

2) The chemical kinetic loss in the scramjet nozzle examined in hot MMH/NTO burning gas was evaluated to be 4.5%. The two-dimensional losses were evaluated to be 16.5% (EN3) and 7% (EN5). The calculated *Isp* agreed with the experimental specific impulse within a discrepancy of 2% for the hot flow. Measurements of the boundary layer for the cold N_2 flow indicated that the boundary layer is turbulent in the scramjet nozzle. The heat transfer measured on nozzles supported this result.

3) Scale effects of thrust of scramjet nozzles were investigated for H_2-fueled scramjets. Chemical kinetic loss, two-dimensional loss and friction loss were found to be approximately equal in full-scale engines with an entrance height of 1 m. The delivered specific impulse of the full-scale scramjet nozzle was estimated to be about 1100 s.

4) The calibrated TDK code showed a strong dependence of lift thrust on nozzle pressure and dimension through chemical kinetics in nozzle flows. The reactive flow in the nozzles can be approximated by partial equilibria between radicals and stable species. This approximation was found to be improved in hypersonic flight situations.

Acknowledgment

This study was conducted as a joint research with Ishikawajima-Harima Heavy Industries, Co. Ltd.

References

[1]Wasko, R. A., "Performance of Annular Plug and Expansion-Deflection Nozzles Including External Flow Effects at Transonic Mach Numbers," NASA TND-4462, April 1968.

[2]Snyder, D. D., and Pinckney, S. Z., "A Configuration Development Strategy for the NASP," International Symposium on Air Breathing Engines 91-7056, Sept. 1991.

[3]Dusa, D. J., "Turboramjet Exhaust Nozzle System," International Symposium on Air Breathing Engines 91-7118, Sept. 1991.

[4]Schetz, J. A., Billig, F. S., and Favin, S., "Numerical Solutions of Scramjet Nozzle Flows," *Journal of Propulsion and Power*, Vol. 3, No. 5, 1987, pp. 440–447.

[5]Sangiovanni, J. J., Barber, T. J., and Syed, S. A., "The Role of Hydrogen/Air Chemistry in Nozzle Performance Simulation for Hypersonic Propulsion Systems," AIAA Paper 90-2492, 1990.

[6]Carpenter, M. H., "The Effects of Finite Rate Chemical Processes on High Enthalpy Nozzle Performance: A Comparison Between "Spark" and "Seagull"," AIAA Paper 88-3157, July 1988.

[7]Harloff, G. J., Redy, D. R., and Lai, H. T., "Viscous Three-Dimensional Analyses for Nozzles for Hypersonic Propulsion," NASA CR-185197, Jan. 1990.

[8]Baysal, O., Engelund, W. C., Eleshaky, M. E., and Pittman, J. L., "Adaptive Computations of Multispecies Mixing Between Scramjet Nozzle Flows and Hypersonic Freestream," AIAA Paper 89-0009, Jan. 1989.

[9]Lai, H., "3D Computation of Hypersonic Nozzle," AIAA Paper 90-5203, Oct. 1990.

[10]Huebner, L. D., and Tatum, K. E., "Computational and Experimental Aftbody Flow Fields for Hypersonic, Airbreathing Configurations with Scramjet Exhaust Flow Simulation," AIAA Paper 91-1709, June 1991.

[11]Flugstad, T. H., Romine, B. M., and Whittaker, R. W., "High Mach Exhaust System Concept Scale Model Test Results," AIAA Paper 90-1905, July 1990.

[12]Re, R. J., and Leavitta, L. D., "Static Internal Performance of Single-Expansion-Ramp Nozzles with Various Combinations of Internal Geometric Parameters," NASA TM-86270, 1984.

[13]Oman, R. A., Foreman, K. M., Leng, J., and Hopkins, H. B., "Simulation of Hypersonic Scramjet Exhaust," NASA CR-2494, March 1975.

[14]Hopkins, H. B., Konpka, W., and Leng, J., "Validation of Scramjet Exhaust Simulation Technique at Mach 6," NASA CR-3003, March 1979.

[15]Waltrup, P. J., Billing, F. S., and Stockbridge, R. D., "A Procedure for Optimizing the Design of Scramjet Engines," *Journal of Spacecraft and Rockets*, Vol. 16, No. 3, 1979, pp. 163–172.

[16]Miyajima, H., et al., "Studies of Scramjet Nozzles; (1) Performance of Two-Dimensional Nozzles," National Aerospace Lab., TR-1149, Japan, April 1992.

[17]Hiraiwa, T., Ueda, S., Sato, S., Mitani, T., Yamamoto, M., and Matsumoto, M., "Off-Design Performance of Scramjet Nozzles," International Symposium on Air Breathing Engines 93-7066, Sept. 1993.

[18]Nakahashi, K., Miyajima, H., Kisara, K., and Moro, A., "A Method to Evaluate Performance of Rockets," National Aerospace Lab., TR-771, Japan, July 1983.

[19]Spalding, D. B., and Chi, S. W., "The Drag of a Compressible Turbulent Boundary Layer on a Smooth Flat Plate with and Without Heat Transfer," *Journal of Fluid Mechanics*, Vol. 18, 1964, pp. 117–143.

[20]"JANNAF Rocket Engine Performance Prediction and Evaluation Manual," JANNAF Interagency Propulsion Committee, Chemical Propulsion Information Agency Publication 246, April 1975.

[21]Miyajima, H., Nakahashi, K., Hirakoso, H., and Sogame, E., "Low-Thrust LO_2/LH_2 Engine Performance with a 300:1 Nozzle," *Journal of Spacecraft and Rockets*, Vol. 22, No. 2, 1985, pp. 188–194.

[22]Kerr, J. A., and Moss, S. J. (ed.), *CRC Handbook of Bimolecular and Termolecular Gas Reactions*, Vol. 1, CRC Press, Boca Raton, FL, 1981.

[23]Jensen, D. E., and Jones, G. A., "Reaction Rate Coefficients for Flame Calculations," *Combustion and Flame*, Vol. 32, 1978, pp. 1–34.

[24]Baulch, D. L., Drysale, D. D., Horne, D. G., and Lloyd, A. C., *Evaluated Kinetics Data for High Temperature Reactions, Vol. II Homogeneous Gas Phase Reactions for System*, CRC Press, Cleveland, OH, 1973.

[25]Davis, D. O., and Gessner, F. B., "Further Experiments on Supersonic Turbulent Flow Development in a Square Duct," *AIAA Journal*, Vol. 27, No. 8, 1989, pp. 1023–1030.

[26]Hopkins, E. J., and Inouye, M., "An Evaluation of Theories for Prediction Turbulent Skin Friction and Heat Transfer on Flat Plates at Supersonic and Hypersonic Mach Numbers," *AIAA Journal*, Vol. 9, No. 6, 1971, pp. 993–1003.

[27]Kehtarnavaz, H., Coats, D. E., and Dang, A. L., "Viscous Loss Assessment in Rocket Engines," *Journal of Propulsion and Power*, Vol. 6, No. 6, 1990, pp. 713–717.

[28]Hedlund, E. R., Higgins, C. W., Rozanski, C. S., Swinford, N. F., and Hills, J. A., "New High Reynolds Number Mach 8 Capability," *AIAA Journal*, Vol. 30, No. 6, 1992, pp. 1665–1667.

[29]Itoh, K., Tani, K., Tanno, H., Takahashi, M., Miyajima, H., and Asano, T., "A Numerical and Experimental Study of Free Piston Shock Tunnel," 19th International Symposium on Shock Waves, Paper 372, Marseille, July 26–30, 1993.

[30]Nickerson, G. R., "Optimized Supersonic Exhaust Nozzles for Hypersonic Propulsion," AIAA/ASME/SAE/ASEE 24th Joint Propulsion Conf., AIAA Paper 88-3161, July 1988.